Trapped Rossby waves

Detlev Müller
Max Planck Institut für Meteorologie, D-20146 Hamburg, Germany
(Received 14 July 1999)

The possibility of tidal dynamics at strictly imaginary Lamb parameters has been known for more than three decades. The present paper explores the prevailing physics in this parameter regime. To this end, basic features of the global circulation such as baroclinicity and geostrophy have to be incorporated into tidal dynamics. The tidal equations of the thermal wind are readily obtained in the framework of spherical bishallow water theory. Density surfaces of a circulation with available potential energy alter the spatial inhomogenities of the generic tidal problem. Wave dynamics in an inhomogeneous medium are characterized not only by a dispersion relation but also by a wave guide geography: significant wave amplitudes are trapped in specific regions of frequency-dependent width. As an inherently global issue, evaluation of the Rossby wave guide geography for a given circulation cannot rely on the familiar regional filters of tidal theory. On the global domain, the Rossby wave specification is given by the Margules filter. A thermal wind is stable against nondivergent Rossby wave disturbances. Rossby waves propagating with a geostrophic wind are governed by prolate dynamics (real Lamb parameters) while imaginary Lamb parameters emerge for the oblate dynamics of Rossby waves running against a geostrophic wind. Oblate Rossby wave dynamics include pole-centered wave guides and very low-frequency disturbances propagating eastward against a westward wind.

PACS number(s): 47.35.+i, 92.10.Hm, 92.60.Dj, 47.32.−y

I. INTRODUCTION

Wave trapping is a classical topic in planetary wave propagation. Historically the first, still approximate solution to Laplace's ''tidal'' equation [1] was Kelvin's equatorially trapped gravity wave [2] which currently plays a central role in intensive studies of the El Nino phenomenon [3,4]. The notion of an ''equatorial wave guide'' was probably first introduced by Yoshida [5] and assumed a definite form with Matsuno's equatorial β-plane approximation [6] of the ''tidal'' equation. On the rotating planet, the curvature of the planetary surface in conjunction with coordinate-dependent Coriolis forces provides an inherently inhomogeneous ''background medium.'' The latitude dependence of metric and Coriolis forces establishes an equator-centered wave guide, the so-called ''Yoshida guide.'' This latitudinal inhomogenity inhibits the communication of wave dynamical imbalances beyond a certain frequency-dependent horizon, the ''critical latitude.'' While wave functions are well approximated by plane waves in the interior of the wave guide, they behave as Airy functions near the critical latitude, oscillating inside the guide and decaying exponentially on its outside [7]. Moreover, topographic large-scale features of the planetary surface such as coasts and mountain ridges lead to topographically trapped waves, the coastally trapped Kelvin wave [8] being perhaps the best known oceanic example.

In addition to these primary factors of planetary wave guide geography, the global circulation of the oceans and the atmosphere itself affects the spatial distribution of trapping regions. A considerable fraction of the intensity and orientation of the global circulation is controlled by pressure forces due to sloping isopycnals, i.e., sloping surfaces of constant density. Differential solar heating induces deviations of isopycnals from equipotential surfaces thus generating the available potential energy [9] of the circulation. A stably stratified, vertically sheared flow of this type is called thermal wind and the wave trapping characteristics of such a circulation are determined by the slope of its isopycnals. With these features wave guide geography is clearly a global issue. While regional approximations apply within a given wave guide such as Matsuno's theory applies inside the Yoshida guide, the determination of the wave guide geography of a circulation has to consider the global domain. In turn, the identification of trapping regions will suggest appropriate approximations valid on these restricted domains. Moreover, wave guide geography will be subject to temporal changes as the climate varies.

Similar to the analysis of hydrodynamic instabilities the evaluation of wave guide geographies considers wave-circulation systems. However, in spite of this common formal framework wave guide geography and stability properties are to be carefully distinguished. For climate dynamics essentially three hydrodynamic instabilities are of greater significance: static (i.e., Rayleigh-Benard) instability of the unstably stratified fluid against internal gravity waves, Kelvin-Helmholtz instability of the stably stratified, vertically sheared fluid against baroclinic gravity waves, and baroclinic instability of the thermal wind against divergent Rossby wave disturbances. Static instability involves fast convective motions on small spatial scales and is generally not explicitly resolved in numerical global circulation models of the ocean and the atmosphere. Rather, its basic role in driving the atmospheric Hadley circulation and the oceanic conveyor belt is taken into account by appropriate parametrizations. Kelvin-Helmholtz instability is associated with a transfer of mean flow kinetic energy to baroclinic gravity waves. Since kinetic energies of terrestrial large-scale circulations are generally small, this instability is considered to be of minor significance for climate variability. In baroclinically unstable systems divergent Rossby waves draw on the available potential energy of the circulation. This process is thought to underly the meandering of the jet stream or the North Atlantic Gulf Stream as well as the generation of eddies in the ocean and the atmosphere. It may also be noted that the development of hurricanes out of tropical Rossby waves is not an instability of this type. Baroclinic instability is considered the primary cause for the chaotic nature of Earth's weather and possibly climate systems and provides the starting point for contemporary theories of geostrophic turbulence.

In the framework of linear stability theory the analysis of these instabilities evaluates the system's dispersion relation and identifies wave growth with the emergence of complex eigenfrequencies. A dispersion relation involves frequencies and wave numbers or wave vectors, but no coordinates. On the other hand, wave guide geography considers the ''wave guide equation.'' This equation is also obtained from the system's wave equation but in contrast to the dispersion relation, it provides an expression for the critical latitude in terms of wave frequencies. In addition, it defines the in- and exterior of the wave guide. As a relation between coordinates and frequencies the wave guide equation does generally not admit conclusions on the system's stability properties.

The appropriate framework for the analysis of wave trapping is given by shallow water theory on the rotating spherical surface. At this time, a large fraction of climate studies is based on Richardson's primitive equations for a Boussinesq fluid near the surface of the rotating sphere [10]. While these equations provide a consistent account of equilibrium circulations and their thermodynamics, they do not pose a Newtonian dynamical problem. The covariant formulation of hydrostatic fluid dynamics is given by shallow water theory. As a vertically integrated approach shallow water theories represent hydrostatic vertical variability as internal variability of an otherwise strictly two-dimensional fluid. The non-Euclidean intrinsic geometry of the spherical surface is accounted for by the nontrivial Riemannian [11]. More than equilibrium problems, spherical shallow waters address issues of motion in the climate system.

Planetary wave dynamics essentially consider linearizations of spherical shallow water theory. The key feature of wave dynamics on the global scale is the spatial variability of geometric and Coriolis coefficients and the basic wave equation on the rotating spherical surface is Laplace's ''tidal'' equation. It may be noted at this point that the name ''tidal'' equation is entirely historical. The significance of Laplace's equation lies primarily in the provision of the fundamental free modes of small amplitude motions on the rotating spherical surface. Furthermore, the application of this equation to a particular (gravitational) forcing at a particular (tidal) frequency certainly does not exhaust its power. Thermally excited tides are a matter of longstanding meteorological interest [12]. Moreover, contemporary satellite altimetry provides records of equatorial and basin-scale ocean waves [13,14] primarily driven by wind and topography. The dynamics of these waves are indeed governed by the ''tidal'' equation. The same applies of course to the tropical ocean waves involved in the El Nino oscillation. While the notion of a ''global'' or ''planetary wave equation'' would be far more appropriate, the historical name will be kept in the following.

Although the wave equation on the global domain is known for more than two centuries, geophysical fluid dynamics discuss wave propagation and wave mean-flow systems essentially in terms of regional approximations such as the f-plane, quasigeostrophic theory or the equatorial β plane. Quasigeostrophic theory is a midlatitude, plane wave approximation which utilizes an approximate version of the tidal wave guide equation as its generic dispersion relation. In fact, the concept has been developed to provide an easy-to-use Cartesian, constant-coefficient algorithm for the analysis of wave-mean flow systems and the detailed study of baroclinic instability. On the other hand, this structure excludes wave trapping issues from the scope of quasigeostrophic theory.

Matsuno's β-plane theory approximates the spherical geometry in the vicinity of the equator in terms of Cartesian coordinates. However, the success of this approach is not primarily based on this simplification. Rather, it is crucial that this approximation is consistent with the wave guide geography of the tidal equation: the Yoshida guide is a definite physical feature of the tidal equation and in the interior of a given wave guide the curvature of the planet's surface is neglible. Moreover, the inherent consistency of Matsuno's approximation with Laplace's equation is emphasized by the existence of various derivations of the concept similar to the variety of arguments leading from the three-dimensional Euler equations to the shallow water approximation. Matsuno's approach is obtained by appropriate assumptions in space-time or in wave number space or in the function space of the tidal equation. It may also be noted that the space-time aspects of the approximation originally go back to Kelvin [2].

The dominance of regional approximations in planetary wave dynamics is essentially due to the complexity of component-wise geometrical considerations in curvilinear coordinates. In the framework of covariant shallow water theory geometrical issues are well understood and the manipulation of basic equations, e.g., the derivation of vorticity and energy budgets or wave equations is straightforward. What remains unsatisfactory though is the analytical side of the theory. Eigenfunctions of planetary wave equations such as Laplace's tidal equation belong to the class of Lamé functions. Unlike functions of the hypergeometric type these functions are only poorly understood. Thus, planetary wave dynamics utilize the combination of analytical and numerical methods. While this approach cannot rely on the formal simplicity of a Cartesian, constant-coefficient framework, it does ensure geometric consistency on the global domain.

In the following, index notation will be used with indices $m,n,\ldots=1,2$ running over longitude λ and latitude φ. In these coordinates the surface metric of a sphere with radius a reads

$$g_{mn}=\begin{vmatrix} a^2\cos^2\varphi & 0 \\ 0 & a^2 \end{vmatrix}$$

while the Levi-Cevita tensor has the form

$$\epsilon_{mn}=a^2(n-m)\cos\varphi.$$

The covariant derivative will be denoted by a semicolon. The componentwise representation of geometrical tensors, Christoffel symbols and further details of tensoranalysis on the spherical surface are given elsewhere [15]. Braced indices $(\ell)=1,2$ refer to the top and bottom layer of the fluid and are not subject to the summation convention. Numerical solutions of Laplace's tidal equation are based on a code developed by Swarztrauber and Kasahara [16] while numerical computations of spheroidal and related wave functions utilize NAG-Lib routine F02GJE.

II. TIDAL EQUATIONS OF THE THERMAL WIND

The stably stratified fluid on the rotating spherical surface will here be represented in terms of spherical bishallow water equations [15]. The idealization of the continuously stratified fluid as a two-layer system is certainly an extreme simplification. However, it does provide a qualitative and consistent model of the dynamics of isopycnals and their interplay with propagating disturbances. The bishallow water equations govern the dynamics of the hydrostatic two-layer fluid with constant, but different layer densities $\rho_{(\ell)}$ and vertically constant, but different layer velocities $V_n^{(\ell)}(t,\lambda,\varphi)$. The layer-mass per unit area is given as

$$R=R_{(1)}+R_{(2)}=\rho_{(1)}H_{(1)}+\rho_{(2)}H_{(2)}$$

with layer thicknesses

$$H_{(1)}=h_0(t,\lambda,\varphi)+h_1(t,\lambda,\varphi),\ \ H_{(2)}=h(\lambda,\varphi)-h_1(t,\lambda,\varphi),$$

where h_0 denotes the free surface, h_1 the layer interface, and h the topographic bottom. All three of these surfaces are assumed to be material surfaces. In this approach, the free surface and layer-interface play the role of isopycnals. The relative magnitude of the top layer is given in terms of the concentration-type variable

$$r=R_{(1)}/R$$

such that $R_{(2)}=(1-r)R$. The system's barycentric mass flux equals the barycentric momentum density (Newton's first law) and is defined as

$$J_n=RV_n=R[rV_n^{(1)}+(1-r)V_n^{(2)}]$$

while the interfacial shear

$$W_n=V_n^{(1)}-V_n^{(2)}$$

determines an additional, baroclinic mass flux

$$I_n=r_{12}RW_n=r(1-r)RW_n\,.$$

In terms of these variables the bishallow water equations are the continuity equation

$$\partial_t R+J^n;_n=0, \tag{2.1}$$

the concentration equation

$$\partial_t Rr+(rJ^n+I^n);_n=0, \tag{2.2}$$

the barycentric momentum budget

$$\partial_t J_n+P^m{}_n;_m=RF_n-\epsilon_{mn}fJ^m, \tag{2.3}$$

and the shear equation

$$D_tW_n+W^mQ_{mn}+\partial_n\mu=0. \tag{2.4}$$

The barycentric momentum flux tensor

$$P_{mn}=J_mV_n+R\Pi_{mn}+Pg_{mn}=P_{nm}$$

is symmetric with respect to the indices m and n and involves a baroclinic stress tensor

$$R\Pi_{mn}=I_mW_n=r_{12}RW_mW_n=R\Pi_{nm}$$

and the effective pressure

$$P=P(R,r)=\frac{1}{2}\gamma_{(2)}(1+\delta r^2)R^2.$$

Here, $\gamma_{(\ell)}=g/\rho_{(\ell)}$ with gravitational acceleration g while

$$\delta=(\gamma_{(1)}-\gamma_{(2)})/\gamma_{(2)}=(\rho_{(2)}-\rho_{(1)})/\rho_{(1)}$$

is the basic stratification parameter of the two-layer fluid. For the stably stratified fluid δ is always positive. The prognostic closure for the baroclinic subsystem is given by the shear equation (2.4) with

$$Q_{mn}=V_n;_m+(1-2r)W_n;_m-W_n\partial_m r+\epsilon_{mn}f,$$

where $f=2\Omega\sin\varphi$ denotes the Coriolis parameter and

$$\mu=\gamma_2\delta(rR+p_*)$$

is an interfacial potential. The shear equation (2.4) represents the covariant, prognostic and nonlinear generalization of the familiar thermal wind equation. External forces included here are given by

$$RF_n=-g(H\partial_n p_*-R\partial_n h)$$

with surface pressure $p_0=gp_*$ and the total layer thickness

$$H=H_{(1)}+H_{(2)}=(1+\delta r)R/\rho_{(2)}\,.$$

With vanishing vertical shear $W_n=0$, the three limits $r=0,r=1$ or $\delta=0$ reduce Eqs. (2.1)–(2.4) to the barotropic one-layer system

$$\partial_t R+J^n;_n=0, \tag{2.5}$$

$$\partial_t J_n+(J^mV_n);_m+\partial_n P=RF_n-\epsilon_{mn}fJ^m, \tag{2.6}$$

where the effective pressure

$$P=P(R)=\frac{1}{2}\gamma R^2$$

with $\gamma=g/\rho$ now is a function of the effective density $R=\rho H$ alone. Moreover, in these limits the external forces

$$F_n=-g\partial_n(p_*/\rho-h)$$

are always expressible in terms of a potential.

In the time-independent limit $(\partial_t=0)$ the shallow water equations admit simple stationary, zonally symmetric $(\partial_\lambda=0)$ solutions on the global domain. For the velocity field

$$V_n=a^2U(\cos^2\varphi,0),$$

where U is constant with the dimension of an angular velocity the momentum budget (2.6) of the one-layer system takes the form

$$a^2(2\Omega+U)U\cos\varphi\sin\varphi=-g\partial_\varphi(h_0+p_*/\rho)$$

indicating that meridional pressure gradients drive this zonal flow. Moreover, the balance involves terms linear in velocity as well as quadratic terms. While the nonlinear terms are decisive for cyclostrophic flows, terrestrial large-scale circulations exhibit velocities which rarely exceed a tenth of the rotation rate. In fact, the feasibility of ''weather prediction by barometer'' and ocean ''circulation estimation by hydrography'' on Earth rests on the simplicity of an essentially linear relationship between wind speeds and ocean currents on one hand and pressure forces on the other. Although the arithmetical contribution of these nonlinear terms is certainly neglible for such geostrophic circulations, they will be kept here. As they do not introduce formal difficulties into present considerations it is not necessary to compromise the geometrical and physical consistency of the solution. In the following, the notion of ''geostrophy'' will be used in reference to the orthogonality of flow and pressure gradients and not necessarily imply a discard of nonlinearities.

Geostrophy is generally considered an extratropical equilibrium, not valid on the global domain. Here, it is seen that the stationary momentum bugdet does not break down in the tropics but calls for a pressure extremum on the equator. Large-scale circulations on this planet exhibit indeed pressure extrema in the vicinity of the equator. However, due to topographic and thermodynamic details of the Earth's surface, these extrema are generally not located on the equator with the rigid geometrical precision required by the above equations. Moreover, this simple geostrophic flow lacks the cellular structure particularly of the atmospheric circulation. With time-independent nondivergent transports it does not involve rising or sinking motion. Essentially, it provides an idealized representation of the basic geostrophic balance on the global domain with the geometrical and physical consistency of spherical shallow waters.

The equilibrium pressure suggests the distinction of two classes of geostrophic flows: flows with constant layer thickness driven by external pressures p_* and flows driven by a meridional gradient in layer thickness. In the first case ($R=\text{const}$) the external surface pressure is of the form

$$p_*=p_*^E-q\sin^2\varphi$$

with the equator-to-pole gradient

$$q=p_*^E-p_*^P=a^2(2\Omega+U)U/2\gamma.$$

Here, the free surface coincides with an equipotential surface and the flow has no available potential energy. This class of solutions represents solid body rotation of the fluid layer.

For the second class of these zonal circulations the external surface pressure p_* is constant and the system possesses available potential energy. This type of solution is of particular interest to geohydrodynamics. The terrestrial climate system is primarily forced by differential solar heating. This forcing provides the direct supply of the global circulation with available potential energy [9]. Hence, these solutions represent a major aspect of the basic forcing mechanism of the global circulation. Stationary, zonal, geostrophic solutions of Eqs. (2.5) and (2.6) with available potential energy assume the form

$$R=R_E-R_0\sin^2\varphi,\quad V_n=a^2U(\cos^2\varphi,0), \qquad (2.7)$$

where $R_0=R_E-R_P$ measures essentially the equator-to-pole gradient of the layer thickness while the constant U satisfies

$$U=-\Omega\pm\sqrt{\Omega^2+2\gamma R_0/a^2}.$$

Expanding the root under the assumption that $\Omega^2\gg 2\gamma|R_0|/a^2$ and choosing the plus sign leads to

$$U\approx\gamma R_0/a^2\Omega$$

as an approximate expression for the flow-speed in the low-velocity limit. This is the usual geostrophic relation of flow amplitude and pressure gradient.

The geostrophic circulation (2.7) is essentially characterized by one nondimensional parameter: the geostrophy parameter

$$b=R_0/R_E=a^2(2\Omega+U)U/2\gamma R_E.$$

This parameter measures the equator-to-pole gradient of the pressure at the bottom of the system and thus the intensity of the zonal flow. It is comparable to Walker's climatological North Atlantic Oscillation (NAO) index measuring the pressure difference between Lisbon and Stykkesholmur (Iceland) and thus the intensity of predominantly westerly winds in the Ferrel cell [17,18]. In the present case the velocity vanishes for constant layer thickness at $b=0$ while the total layer thickness at the poles becomes zero for $b=1$. Geostrophy parameters larger than one indicate that the fluid occupies less than the entire globe. Such cases will not be considered in the following. It is emphasized that the possibility of finite available potential energy for this barotropic system rests essentially on the free surface. With a rigid lid the quantity R_0 and thus the geostrophy parameter b will always vanish.

The Lagrangian of Eqs. (2.5) and (2.6) is invariant with respect to particle relabeling and by Noether's theorem the system thus conserves potential vorticity following particle trajectories. For the present geostrophic flow the potential vorticity is given by

$$RZ=\epsilon^{an}V_{n;a}+f=2(\Omega+U)\sin\varphi. \qquad (2.8)$$

In the low-velocity limit this reduces to the familiar approximation $Z\approx f/R$. The potential vorticity gradient assumes the form

$$R^2\partial_n Z=2(\Omega+U)R_E(1+b\sin^2\varphi)(0,\cos\varphi). \qquad (2.9)$$

Quasigeostrophic stability considerations suggest that a sign change of the potential vorticity gradient is a necessary condition for instability [19]. Here, it is seen that such a zero crossing may occur for westward flows with $b<-1$. This indicates a fundamental difference in the stability properties of eastward and westward flows of the type (2.7): for westward flows the stabilizing effect of the eastward rotation decreases.

Both of these types of geostrophic flows are readily generalized to bishallow water. Of primary interest here is the thermal wind, i.e., a stably stratified, vertically sheared geostrophic flow with available potential energy. The corresponding stationary, zonally symmetric solution of Eqs. (2.1)–(2.4) takes the form

$$R=R_E-R_0\sin^2\varphi,\quad R_{(1)}=R_E^{(1)}-R_0^{(1)}\sin^2\varphi, \tag{2.10}$$

$$V_n=a^2U(\cos^2\varphi,0),\quad W_n=a^2W(\cos^2\varphi,0), \tag{2.11}$$

where

$$U=rU_{(1)}+(1-r)U_{(2)},\quad W=U_{(1)}-U_{(2)}$$

with constant $U_{(\ell)}$ while $R_0=R_E-R_P$ and $R_0^{(\ell)}$, respectively, denote the equator-to-pole gradient of the corresponding quantity. The surface pressure p_* is here assumed to be constant and for finite R_0 and $R_0^{(\ell)}$ neither the free surface nor the interface coincide with equipotential surfaces. For the flow amplitude one finds from the stationary momentum budgets (2.3) and (2.4)

$$\vartheta_{(1)}=a^2(2\Omega+U_{(1)})U_{(1)}=2\gamma_{(2)}(R_0+\delta R_0^{(1)}),$$

$$\vartheta_{(2)}=a^2(2\Omega+U_{(2)})U_{(2)}=2\gamma_{(2)}R_0.$$

Neglecting the nonlinear terms this yields the shear approximation

$$W\approx(\vartheta_{(1)}-\vartheta_{(2)})/2a^2\Omega\approx\gamma_{(2)}\delta R_0^{(1)}/a^2\Omega$$

in the low-velocity limit. This is the thermal wind relation in the narrow sense: the vertical shear of the geostrophic flow is determined by stratification and the meridional gradient of the hydrostatic pressure at the layer interface h_1. The thermal wind circulation [Eqs. (2.10), (2.11)] is characterized by two nondimensional parameters. The geostrophy parameter

$$b=R_0/R_E=a^2(2\Omega+U_{(2)})U_{(2)}/2\gamma_{(2)}R_E$$

measures again the meridional pressure gradient at the bottom of the system and thus the intensity of the zonal flow in the bottom layer. The baroclinicity parameter

$$b^{(1)}=R_0^{(1)}/R_E^{(1)}=(\vartheta_{(1)}-\vartheta_{(2)})/2\gamma_{(2)}\delta R_E^{(1)}$$
$$\approx a^2\Omega W/\gamma_{(2)}\delta R_E^{(1)}$$

measures the meridional pressure gradient at the layer interface and thus the vertical shear of the circulation. The parameter $b^{(1)}$ vanishes if the system is shear-free and assumes values larger than one if the bottom layer outcrops at some latitude so that the fluid poleward of this latitude is only a one-layer system. Outcrops will not be considered in the following.

A key feature of the bishallow water equations (2.1)–(2.4) is the layer-wise conservation of potential vorticity in the absence of external forcing, while the barycentric potential vorticity is generally not conserved due to baroclinic vorticity sources. By Noether's theorem, the Lagrangian of bishallow water is hence invariant under intralayer relabeling of fluid particles but generally not under inter-layer relabeling. For the barycentric potential vorticity Z of the thermal wind (2.10), (2.11) one obtains

$$RZ=\epsilon^{an}V_n{;}_a+f=2(\Omega+U)\sin\varphi+\epsilon^{an}W_n\partial_a r$$

involving additional contributions from the system's vertical variability in terms of the cross product of vertical shear and concentration gradient. In terms of layer vorticities the barycentric vorticity reads

$$RZ=R[r^2Z_{(1)}+(1-r)^2Z_{(2)}]+\epsilon^{an}W_n\partial_a r.$$

This expression indicates that unlike the barycentric momentum density potential vorticity is not an additive quantity.

The small-amplitude dynamics on the thermal wind are now obtained by linearization of the bishallow water equations (2.1)–(2.4) around the exact solution (2.10), (2.11). This linearization is identical with standard procedures in linear stability theory. In the present case the steady flow (R,r,J_n,I_n) is superposed by small amplitude disturbances (m,η,j_n,i_n). The physical interpretation of these perturbations is given by their relation to the corresponding small amplitude disturbances $(m_{(\ell)},v_n^{(\ell)})$ of the layer variables $(R_{(\ell)},V_n^{(\ell)})$:

$$m_{(1)}=rm+R\eta,$$

$$m_{(2)}=m-m_{(1)},$$

and

$$j_n=R(v_n-\eta W_n)=R[rv_n^{(1)}+(1-r)v_n^{(2)}]=j_n^{(1)}+j_n^{(2)},$$

$$i_n=r_{12}Rw_n=r_{12}R(v_n^{(1)}-v_n^{(2)})=(1-r)j_n^{(1)}-rj_n^{(2)}.$$

Here, $m_{(2)}$ represents vertical disturbances of the layer interface while $m_{(1)}$ measures the joint perturbation due to vertical displacements of the interface and the free surface. The barycentric and baroclinic momentum perturbations are simple linear combinations of the corresponding layer quantities. For sufficiently brief time intervals the amplitudes of such disturbances will remain small and their dynamics are governed by the linearization of the bishallow water equations (2.1)–(2.4) around Eqs. (2.10), (2.11)

$$d_0m+j^n{;}_n=-RW^n\partial_n\eta, \tag{2.12}$$

$$Rd_1\eta+i^n{;}_n=-r_{12}W^n\partial_n m-j^n\partial_n r, \tag{2.13}$$

$$d_0j_n+\epsilon_{mn}Fj^m+\gamma_{(2)}R\partial_n m+\mu\partial_n m_{(1)}$$
$$=-W^m\partial_m i_n-2\epsilon_{mn}Si^m, \tag{2.14}$$

$$d_1i_n+\epsilon_{mn}F_1i^m+(1-r)\mu\partial_n m_{(1)}$$
$$=-r_{12}(W^m\partial_m j_n+2\epsilon_{mn}Sj^m). \tag{2.15}$$

Equations (2.12)–(2.15) are the tidal equations of the thermal wind. These equations are globally valid and geometric approximations are not involved. Advection in the barycentric and baroclinic subsystems are due to different mean flow velocities and

$$d_0=\partial_t+U\partial_\lambda\,,\quad d_1=\partial_t+u\,\partial_\lambda$$

denote the corresponding partial substantial derivatives with baroclinic advection velocity

$$u=(1-r)U_{(1)}+rU_{(2)}\,.$$

Similarly, one has for the effective Coriolis parameters

$$F=rF_{(1)}+(1-r)F_{(2)}\,,\quad F_1=(1-r)F_{(1)}+rF_{(2)}$$

with $F_{(\ell)}=2(\Omega+U_{(\ell)})\sin\varphi=R_{(\ell)}Z_{(\ell)}$ for individual layers and

$$2S=F_{(1)}-F_{(2)}=2W\sin\varphi.$$

The representation of the linearized pressure forces in terms of $(m,m_{(1)})$ has been chosen for convenience and transition to the (m,η) representation is a matter of simple algebra.

In spite of its idealization and linearity the system (2.12)–(2.15) addresses a wide range of phenomena which are currently considered essential to climate dynamics. These include the propagation of barotropic and (first mode) baroclinic gravity and Rossby waves as well as linear stability theory for geostrophic circulations on the rotating spherical surface. Hence, Eqs. (2.12)–(2.15) determine stability thresholds and growth rates for static, Kelvin-Helmholtz and baroclinic instability. The quasigeostrophic approximation to Eqs. (2.12)–(2.15) is given by Phillip's two-layer model [20] and in the limit of vanishing mean available potential energy, the system has been used to evaluate the Kelvin-Helmholtz instability condition on the rotating spherical surface [21]. Here, it is of particular interest that Eqs. (2.12)–(2.15) also determines the wave guide geography of the thermal wind [Eqs. (2.10), (2.11)] and the system will hence be used to determine the distribution of trapping regions for Rossby waves.

III. GLOBAL ROSSBY WAVES

The specification to Rossby waves calls for the definition of a Rossby wave filter for the tidal equations of the thermal wind (2.12)–(2.15) which applies on the global domain. This will here be evaluated in the framework of the one-layer limit of Eqs. (2.12)–(2.15). In this case the perturbation dynamics reduce to

$$d_t m+j^n;_n=0 \tag{3.1}$$

$$d_t j_n+\epsilon_{mn}Fj^m+\gamma R\,\partial_n m=0. \tag{3.2}$$

These equations are also obtained by linearization of the barotropic shallow water equations (2.5), (2.6) around the stationary, geostrophic circulation (2.7). With the mean flow potential vorticity Z given by Eq. (2.8) the perturbation potential vorticity z of the one-layer system is defined as

$$Rz=\epsilon^{an}v_n;_a-Zm.$$

The budget of this quantity is obtained by taking the curl of Eq. (3.2)

$$Rd_t z+j^a\partial_a Z=0, \tag{3.3}$$

where the mean potential vorticity gradient of the barotropic mean flow is given by Eq. (2.9). For the positive definite perturbation energy

$$e=\frac{1}{2}v^n v_n+\gamma m^2/2R,$$

Eqs. (3.1) and (3.2) yield the budget

$$R\partial_t e+(eJ^n+s^n);_n=0$$

with Poynting vector

$$s_n=\gamma m j_n$$

indicating that perturbation energy is conserved in the sense of Gauss' theorem. The system (3.1) and (3.2) governs the dynamics of small-amplitude disturbances of a barotropic geostrophic circulation with available potential energy. If the geostrophy parameter b and thus the available potential energy vanishes Eqs. (3.1) and (3.2) reduces to Laplace's tidal equations. In this case

$$\gamma R=gH=c^2=\text{const},$$

where c denotes the intrinsic phase speed of the barotropic one-layer system. In the strict sense the mean flow velocity U also vanishes in this limit which constitutes the generic tidal problem.

The generic tidal equations pose the fundamental wave propagation problem on the global domain and thus are the starting point of wave-circulation theory. Although these equations are known for more than two centuries the complete analytical solution of this linear problem is still not available. Tidal eigenfunctions belong to the class of doubly periodic or Lamé functions. Physically, tidal dynamics consider wave propagation in an inhomogeneous and anisotropic medium. The primary sources of inhomogenity are the curvature of the planetary surface and the Coriolis forces. Since both, metric and Coriolis forces only depend on latitude, zonal wave dynamics differ significantly from those in meridional direction. Due to this anisotropy tidal eigenfunctions are of the form

$$e^{-i(\omega t-M\lambda)}F(y;N,M) \tag{3.4}$$

with frequency ω, zonal wave number M, mode number N, and $y=\sin\varphi$. Solutions of this type propagate only in the zonal direction and do not involve meridional propagation. In this framework all phase as well as group velocities are exclusively zonal. Moreover, zonal variations are well represented by plane waves. For the standing meridional wave this is not the case. The latitudinal inhomogenities of the rotating spherical surface prevent the communication of wave dynamical imbalances beyond a certain critical latitude and waves are trapped in zonally oriented, channel-like wave guides. Near the critical latitude, meridional wave functions behave as Airy functions, oscillating inside the wave guide and decaying exponentially on its outside. The width of the wave guide is determined by the inhomogenities of the medium as well as the kinematics of the wave. Thus, latitudinal inhomogenity introduces a pronounced regionalization of wave activity on the rotating spherical surface. The wave guide geography of the tidal problem and generally of all wave-circulation systems is the global distribution of trapping regions given by the central and critical latitudes of all wave guides.

The wave guide geography of the nonrotating planet depends on the curvature of the spherical surface and—since poles are arbitrary—on the frequency and propagation direction of the wave. On the rotating planet rotation introduces a genuine anisotropy and wave guides are zonally oriented. For the generic tidal problem the (nondimensional) Lamb parameter

$$\alpha = 2a\Omega/c$$

provides the basic measure of the ratio of the rotation velocity and the intrinsic phase speed of the wave. On Earth, this parameter assumes a wide range of values. For given Earth radius a and rotation rate Ω variations of the Lamb parameter express variations of the intrinsic phase speed c. In the following, reference to baroclinic modes in conjunction with the barotropic one-layer system implies the ''reduced gravity'' or ''equivalent height'' interpretation of Eqs. (3.1)–(3.3). The Lamb parameter vanishes in two distinct limits: either the planet does not rotate ($\Omega = 0$) or the waves are nondivergent ($c \to \infty$). For barotropic modes in the troposphere it assumes values $\alpha \approx 3$ while $\alpha \approx 60$ for tropospheric first baroclinic modes. In the ocean, $\alpha \approx 5$ in the barotropic case and $\alpha \approx 300$ for waves in the first baroclinic mode. The Lamb parameter controls the trapping characteristics of tidal eigenfunctions. With the eigenfunctions of the tidal problem, its (nondimensional) eigenfrequencies

$$\nu = a\omega/c = \nu(N,M;\alpha)$$

also depend on the Lamb parameter. In addition to the spectrum, wave dynamics in an inhomogeneous medium determine the wave guide geography in terms of the critical latitude

$$y_{\mathrm{cr}} = y_{\mathrm{cr}}(\nu, M;\alpha)$$

and the central latitude of the guide.

The comprehensive numerical solution of the generic tidal problem has been given by Longuet-Higgins [22]. Essential features of these tidal eigenfunctions are shown in Fig. 1. In addition to the trapped solutions shown in Fig. 1(a) the tidal equation also has untrapped solutions oscillating on the entire domain. If waves are trapped the central latitude of the wave guide is the equator. The generic tidal problem only admits the equator-centered Yoshida guide. This wave guide is by no means a narrow, tropical channel: with decreasing Lamb parameter the Yoshida guide extends to moderate and even high latitudes. Similar to Airy functions the amplitude of tidal eigenfunctions increases towards the critical latitude.

The solid lines in Figs. 1(b) and 1(c) show tidal eigenfrequencies obtained from the numerical solution of the generic tidal equations (3.1) and (3.2). Fig. 1(b) is the ''Lamb representation'' $\nu = \nu(\alpha, N; M)$ of the dispersion relation at fixed zonal wave number M while Fig. 1(c) gives the ''Matsuno representation'' $\nu = \nu(N,M;\alpha)$ at fixed Lamb parameter. For the Matsuno representation it is noted that the linkage of eastern and western branches into one mode is not a unique operation since tidal eigenfrequencies ν depend only on integer N and M. For the left ($\alpha = 3$) panel of Fig. 1(c) the Margules convention has been chosen while the middle ($\alpha = 30$) and right ($\alpha = 300$) panel follow the Matsuno convention. Both Figs. 1(b) and 1(c) exhibit the characteristic east-west asymmetry of the tidal spectrum. Gravity waves propagate to the east as well as to the west and the lowest eastward gravity mode is the Kelvin wave. For the generic tidal problem low-frequency Rossby waves propagate exclusively to the west. Both wave types are seperated by the Yanai wave which behaves Rossby-like at small values of α and gravitylike at large Lamb parameters [23,24].

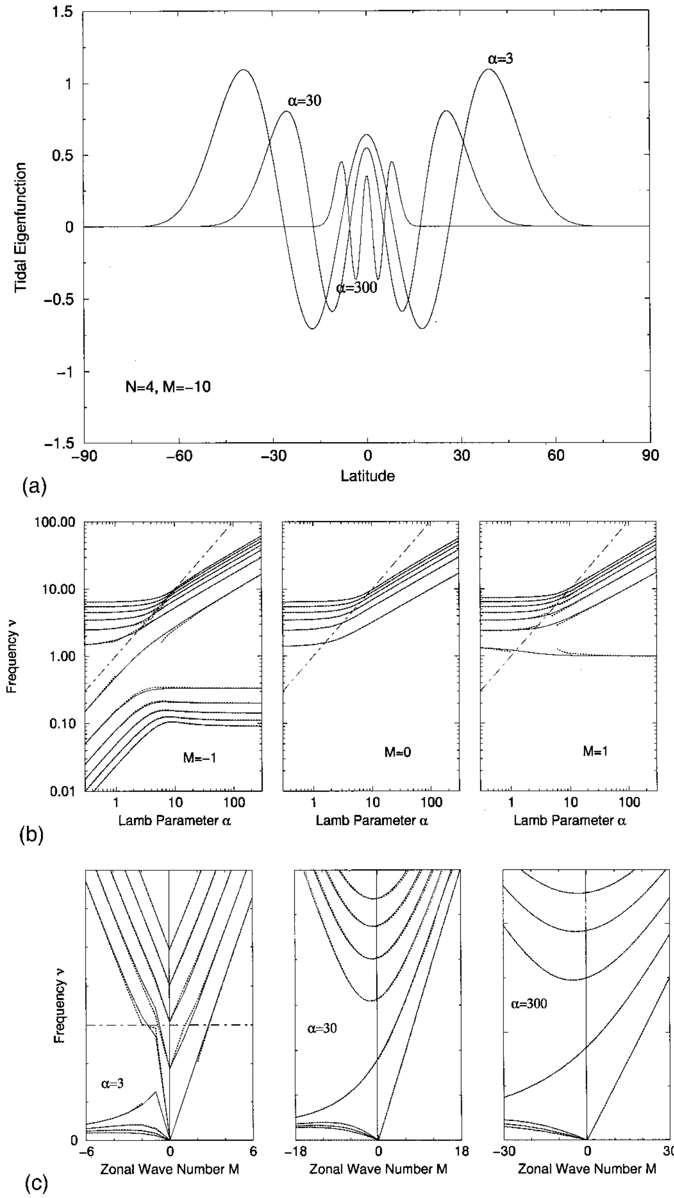

FIG. 1. (a) Tidal eigenfunctions. Mass flux j_2 for Rossby wave with $N=4$, $M=-10$ at Lamb parameters $\alpha = 3,30,300$. (b) Tidal dispersion relation, Lamb representation. Solid lines: numerical solution of Eqs. (3.1) and (3.2) at $b=0$. Dotted lines, left and right panel: (3.8) and (3.10). Dotted lines, middle panel: (3.7). Dashed-dotted line: $\nu = \alpha$. (c) Tidal dispersion relation, Matsuno representation. Solid lines: numerical solution of Eqs. (3.1)and (3.2) at $b=0$. Dotted lines: (3.8) and (3.10). Dashed-dotted line: $\nu = \alpha$.

On the basis of dispersive features of gravity waves on an

f plane (Poincaré waves) it is often assumed that there are no gravity waves with frequencies below f. In tidal theory the quantity corresponding to the Coriolis parameter of the f-plane approximation is the Lamb parameter α. In the dispersion diagrams 1(b) and 1(c) the dashed-dotted line marks frequencies $\nu=\alpha$. While it is obvious that the generic tidal problem does not admit Rossby waves with frequencies higher than α, it is also seen that there are numerous gravity modes with frequencies $\nu<\alpha$. This is clearly the case at those large values of the Lamb parameter that are relevant for baroclinic ocean waves. Only at very small values of α do all gravity frequencies exceed the Lamb parameter. In tidal theory the seperation of gravity and Rossby modes is not provided by the Coriolis parameter but by the Yanai mode assuming a similar role as the well known Lamb wave between internal gravity waves and acoustic modes. Moreover, the Matsuno representation for $\alpha=300$ corresponds quantitatively most closely to the set of first baroclinic modes observed in the ocean. This diagram is frequently associated with ''tropical waves'' in view of the small width of the corresponding Yoshida guide. However, it is emphasized that extratropical features of the generic tidal eigenfunctions do not introduce additional or qualitatively different dispersion properties. This is seen in Fig. 1(c) from the Matsuno diagrams for $\alpha=3$ (corresponding approximately to barotropic modes in the ocean and the troposphere) and for $\alpha=30$ (corresponding approximately to first baroclinic modes in the troposphere): both diagrams exhibit qualitatively the same structure. What does differ at these parameter values is the width of the Yoshida guide extending to moderate and high latitudes. In this sense the Matsuno diagram provides a qualitatively complete picture of the generic tidal dispersion properties. Unlike wave propagation in homogeneous media the tidal dispersion relation does not suggest that all disturbances populate all of the globe nor does it provide information on the regions populated by specific disturbances. The issue of geographical distribution of waves is addressed by the wave guide equation.

Interestingly enough the numerical solution of the tidal problem did not initialize extensive studies of wave-circulation systems on the global domain during the three decades since its publication. Currently, issues of dynamical stability of the climate system are exclusively discussed on the basis of regional approximations such as Matsuno's theory or the quasigeostrophic approximation. These approaches provide approximate analytical expressions for the corresponding dispersion relation and, in the case of Matsuno's theory, the wave guide equation. Expressions of this type admit quite general conclusions on the modification of wave propagation and trapping due to mean flows as well as the mean flow response to small amplitude disturbances. Although the complete analytical solution of the generic tidal problem is not available at this time there are exact analytical solutions in special cases and analytical approximations covering the entire wave number space of the tidal equation. These elements of the complete analytical solution do provide a basis for the analysis of aspects of propagation, trapping, and wave circulation interplay on the global domain as well as the identification of well-defined Rossby wave filters.

In the following a finite circulation velocity U will be reintroduced while keeping the geostrophy parameter at zero. This inclusion of solid body rotation generalizes the kinematics of the generic tidal problem with respect to the relation of advection, Doppler shift and the modification of the Coriolis parameter. One wave equation of the tidal problem is obtained by taking the divergence of Eq. (3.2) and eliminating the perturbation momentum with the result

$$(d_t^2+F^2)[(d_t^2+F^2-c^2\Delta)d_t+c^2\epsilon^{mn}F_n\partial_m]m \\ =-c^2D^{mn}\partial_m F^2\partial_n m, \tag{3.5}$$

where

$$D^{mn}=g^{mn}d_t+\epsilon^{mn}F.$$

This equation governs all waves involving a finite mass perturbation. However, since the tidal problem also admits nondivergent Rossby waves, the null space of Eq. (3.5) contains nontrivial solutions. These are explicitely included in the more general vector wave equation which follows from taking the time-derivative of Eq. (3.2) and eliminating the mass perturbation

$$(d_t^2+F^2-c^2\underline{\Delta})d_t j_n+c^2\epsilon_{na}[\partial^a(F^b j_b)+F^a j^b{}_{;b}]=0$$

with

$$\underline{\Delta} j_n=g^{ab}j_{n;ab}-G_{an}j^a=\left(\Delta-\frac{1}{a^2}\right)j_n,$$

where $G_{an}=a^{-2}g_{an}$ denotes the Ricci tensor of the spherical surface [21]. This vector wave equation is the general tidal wave equation. A useful auxiliary wave equation is obtained by multiplying it with the gradient of the Coriolis parameter and using the vorticity budget (3.3). For vanishing geostrophy parameter the vorticity budget reduces to

$$j^a F_a=-R^2 d_t z$$

and one obtains from the vector wave equation above

$$R^2[(d_t^2+F^2-c^2\Delta)d_t+c^2\epsilon^{mn}F_m\partial_n]z=c^2(\Delta F)j^n{}_{;n}. \tag{3.6}$$

Since Eq. (3.6) involves vorticities and divergencies it is clearly not a closed equation. However, if the Laplacian of the Coriolis parameter is neglibly small (essentially inside the Yoshida guide) or the disturbances are only weakly divergent equation (3.6) is seen to provide a fairly simple, yet globally valid approximation for waves with finite potential vorticity. In essence, (3.6) is the spherical generalization of Matsuno's wave equation on the equatorial β-plane. In the following (3.6) will hence be addressed as the ''spherical Matsuno equation'' or simply as the Matsuno equation.

Adopting the separation ansatz (3.4) for the mass perturbation m, equation (3.5) becomes

$$(1-\tau^2y^2)(\Delta-\alpha^2y^2+\nu^2-\tau M)m \\ =-2[\tau^2(1-y^2)y\partial_y+\tau M]m,$$

where

$$\tau=\alpha/\nu=2(\Omega+U)/(\omega_0-UM)$$

and ν now denotes the (nondimensional) Doppler-shifted frequency

$$\nu = a\omega/c = a(\omega_0 - UM)/c$$

with the frequency ω_0 (of dimension 1/sec) seen by an observer rotating with the planet while

$$\alpha = 2a|\Omega + U|/c$$

is the modified (nondimensional) Lamb parameter and the inequality $|U| \ll \Omega$ always holds for large-scale flows on Earth. For the Matsuno equation the divergence can be eliminated using the equations of motion (3.1)–(3.3) and the separation ansatz (3.4) yields

$$(1-qy^2)(\Delta - \alpha^2 y^2 + \nu^2 + \tau M)z = -2[q(1-y^2)y\partial_y - \tau M]z$$

with

$$q = \nu^2/(\nu^2 - M^2).$$

In special cases, exact analytical solutions to these equations are known in terms of prolate spheroidal wave functions [25,26]. In addition to the mode and zonal wave numbers these functions depend on the Lamb parameter α: at small values of α they behave as Legendre functions while they resemble Hermite polynominals at large Lamb parameters. Details of spheroidal wave functions are given in the Appendix. Known exact analytical solutions [27,28] of the tidal problem satisfy the dispersion relation

$$\nu^3 - \epsilon_P(N, M-1; \alpha)\nu - \alpha M = 0, \qquad (3.7)$$

where ϵ_P denotes the prolate spheroidal eigenvalue. This dispersion relation is exactly valid at $\Omega + U = 0$ (nonrotating gravity waves), $\nu = \alpha$ (M_2-tide, the principal lunar tidal signal), $M = 0$ (standing waves) and $c \to \infty$ (nondivergent Rossby waves). While (3.7) is an exact analytical result for these four special classes it does remain a limitation that a closed expression for ϵ_P as function of its arguments is not known. In practice (3.7) is exploited with the help of power series and asymptotic expansions for $\epsilon_P(\alpha)$ as well as numerical solutions of the prolate spheroidal wave equation. For standing waves ($M = 0$) solutions of (3.7) based on numerical computations of $\epsilon_P(N,1;\alpha)$ are seen in the middle panel of Fig. 1(b).

The trapping characteristics of tidal eigenfunctions are defined by the existence of a critical latitude in the vicinity of which the function exhibits Airy-type behavior. This critical latitude follows directly from the wave equation. For standing waves ($M = 0$) the Matsuno equation reduces to

$$[(1-y^2)\partial_y^2 - \alpha^2 y^2 + \nu^2]z = 0$$

indicating that an Airy approximation holds in the vicinity of

$$y_{\rm cr}^2(M=0) = \nu^2/\alpha^2 = \omega_0^2/4(\Omega + U)^2$$

and is of the form

$$[(1-y_{\rm cr}^2)\partial_x^2 - W_{\rm cr}x]z \approx 0,$$

where $x = y - y_{\rm cr}$ and $W_{\rm cr} = 2\alpha^2 y_{\rm cr}$. Since always

$$W_{\rm cr}x < 0 \quad \text{for} \quad y^2 < y_{\rm cr}^2$$

standing waves oscillate equatorwards of the critical latitude and decay exponentially towards the pole. Thus, standing gravity waves with frequencies $\nu < \alpha$ are trapped in the equator-centered Yoshida guide with a width inversely proportional to the Lamb parameter. Standing gravity waves with frequencies higher than α are not subject to wave trapping. Moreover, it is seen that an eastward circulation ($U > 0$) narrows the wave guide while a westward circulation ($-\Omega < U < 0$) widens it. Similarly one finds the wave guide equation for nonrotating gravity waves

$$y_{\rm cr}^2(\Omega + U = 0) = (\nu^2 - M^2)/\nu^2$$

or using the dispersion relation (3.7)

$$y_{\rm cr}^2(\Omega + U = 0) = \Lambda/(\Lambda + M^2)$$

with

$$\Lambda(N,M) = N(N+1) + (2N+1)|M|.$$

This expression indicates that trapping due to the surface curvature alone affects primarily waves with large zonal wave numbers, i.e., zonally short waves. For the M_2 tide with $\nu = \alpha$ one obtains

$$\alpha^2 y_{\rm cr}^4 - (2\alpha^2 - M)y_{\rm cr}^2 + \alpha^2 - M^2 + M = 0$$

and for nondivergent Rossby waves

$$y_{\rm cr}^2(c \to \infty) = 1 + \sigma M,$$

where $\sigma = 1/\tau$. In this case, the dispersion relation (3.7) yields

$$y_{\rm cr}^2(c \to \infty) = \Lambda/(\Lambda + M^2)$$

demonstrating the close resemblance of the trapping characteristics of nondivergent Rossby waves and nonrotating gravity waves. In general, wave guide equations admit complex solutions. However, such roots do not indicate an instability of the underlying and in the present case trivial ground state, but simply an absence of wave trapping. Physical solutions to wave guide equations are necessarily confined to the real interval $[-1,1]$. Unlike the dispersion relation, wave guide equations yield information on the regionalization of small-amplitude perturbations.

In addition to these exact solutions the wave equations (3.5), (3.6) suggest various approximations which provide an overview of the entire wave number space of the tidal equation. Of particular interest here is the Matsuno equation (3.6). Inside the Yoshida Guide or for weakly divergent waves this equation reduces essentially to

$$(\Delta - \alpha^2 y^2 + \nu^2 - \tau M)z \approx 0.$$

This approximation is a globally defined prolate spheroidal wave equation. Prolate spheroidal solutions of the approximate Matsuno equation are shown in Fig. 2. In comparison to Fig. 1(a) it is seen that these functions qualitatively as well as quantitatively capture all features of tidal eigenfunctions. In fact, the degree of agreement between the numerical solutions and these spheroidal approximations suggests that the

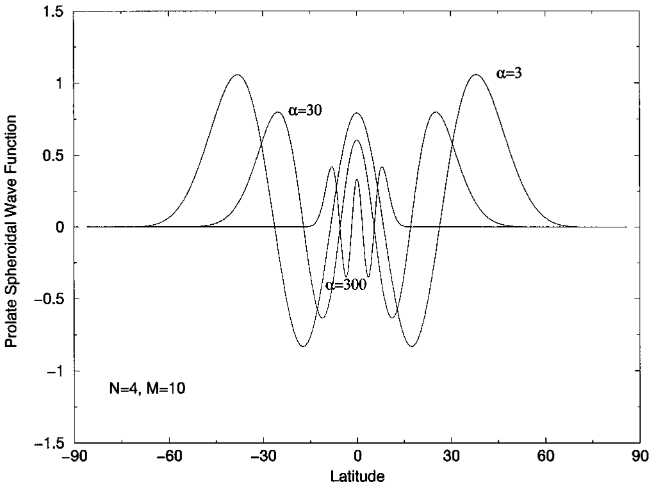

FIG. 2. Prolate spheroidal wave function. For $N=4$, $M=10$ at Lamb parameters $\alpha=3{,}30{,}300$.

complete analytical solution of the tidal equation can be expressed in terms of prolate spheroidal wave functions.

The dispersion relation of the approximate Matsuno equation follows as

$$\nu^3-\epsilon_P(N,M;\alpha)\nu-\alpha M\approx 0 \tag{3.8}$$

while the wave guide equation becomes in this case

$$\nu^3\approx\left(\frac{M^2}{1-y_{\rm cr}^2}+\alpha^2 y_{\rm cr}^2\right)\nu+\alpha M. \tag{3.9}$$

Similarly, one finds for high-frequency gravity waves with $\nu>\alpha$ a spheroidal approximation with dispersion relation

$$\nu^3-\epsilon_P(N,M;\alpha)\nu+\alpha M\approx 0. \tag{3.10}$$

Using numerically computed prolate spheroidal eigenvalues, the eigenfrequencies (3.8) and (3.10) are shown as dashed lines in Fig. 1. Frequencies $\nu>\alpha$ and the Kelvin frequencies at large α are obtained from Eq. (3.10) while other low frequencies $\nu<\alpha$ of gravity and Rossby waves are calculated with Eq. (3.8). It is seen from Fig. 1 that these spheroidal approximations generally represent tidal eigenfrequencies satisfactorily. However, gaps in the dotted lines for the Kelvin and Yanai waves at moderate Lamb parameters indicate that the approximations (3.8) and (3.10) break down in this parameter range. For $N=0$, small M and moderate Lamb parameters

$$(\epsilon_P/3)^3<(\alpha M/2)^2$$

so that two of the roots of Eq. (3.8) and two of the roots of Eq. (3.10) become complex. Since it is known from the numerical solution that all eigenfrequencies are real this inequality indicates the invalidity of the simple spheroidal approximations to Eqs. (3.5), (3.6) in this parameter range. In these cases the right hand sides of Eqs. (3.5), (3.6) are not neglible. In a small and restricted domain of wave number space the spheroidal approximation to the wave equations (3.5), (3.6) is thus inconclusive with respect to stability.

In spite of this applicability restriction, these formulas generalize various well known approximations of geophysical fluid dynamics. The dispersion relation (3.8) provides a common basis for modes with finite potential vorticity. At large intrinsic phase speeds ($c\to\infty$) this relation reduces to the exact solution (3.7)

$$\omega_0=UM-2(\Omega+U)M/L(L+1),$$

where $L=N+|M|$. This is Margules' classical result for nondivergent Rossby waves [27]. In the large-c limit the wave guide equation (3.9) becomes

$$y_{\rm cr}^2=1+\sigma M$$

in agreement with the previously obtained exact expression. Furthermore, using the asymptotic expansion (see Appendix) for the prolate eigenvalue at large values of the Lamb parameter (3.8) becomes

$$\nu^3-[\alpha(2N+1)+M^2]\nu-\alpha M\approx 0.$$

This is the familiar dispersion relation of Matsuno's equatorial β-plane theory [6,8]. Inserting this dispersion relation into the wave guide equation (3.9) one finds

$$y_{\rm cr}^2\approx(2N+1)/\alpha,$$

the classical expression for the Yoshida Guide of Matsuno's β-plane theory [8]: at large values of the Lamb parameter the width of the wave guide is independent of the zonal wavelength. Solid body rotation merely modifies the width of the Yoshida Guide: an eastward circulation narrows it while a westward circulation widens it.

The Matsuno wave guide equation (3.9) also provides a direct link to readily observable large-scale disturbances in the ocean-atmosphere system. Setting

$$k=M/a\cos\varphi,\quad F=2(\Omega+U)\sin\varphi,\quad \beta=2(\Omega+U)\cos\varphi/a$$

this equation assumes the form

$$C^3(y_{\rm cr})=(c^2+F_{\rm cr}^2/k^2)C(y_{\rm cr})+c^2\beta_{\rm cr}/k^2$$

with $C(y_{\rm cr})=\omega/k$. For gravity waves this expression is sufficiently approximated by

$$C_G^2(y_{\rm cr})\approx c^2+F_{\rm cr}^2/k^2$$

stating that at the same zonal wavelength trapped gravity waves with wide Yoshida guides are faster than gravity waves with narrow guides. A corresponding eastward propagating wave front is frequently observed as atmospheric teleconnection pattern in conjunction with El Nino [29]. Over the Pacific this pattern is enhanced by low-latitude trades and midlatitude westerlies. It is furthermore seen that this approximation closely resembles the familiar f-plane dispersion relation. However, it is emphasized that f-plane dynamics only approximate the zonal features of tidal dynamics and do not account for the anisotropy of the rotating spherical surface. Tidal functions which approximately satisfy this dispersion relation (rather, wave guide equation) do not behave as plane waves in the meridional direction. This interpretation also clarifies the absence of Poincaré waves with frequencies below F: tidal gravity modes with lower frequencies or slower zonal phase speeds are trapped in narrower wave guides and do not exhibit a significant amplitude at the latitude given by $F_{\rm cr}$.

For Rossby waves, $C_R^3(y_{\rm cr})$ is neglibly small and the Matsuno wave guide equation is sufficiently approximated by

$$C_R(y_{\rm cr}) \approx -c^2\beta_{\rm cr}/(c^2k^2+F_{\rm cr}^2)$$

stating that at the same zonal wavelength trapped Rossby waves with wide Yoshida guides are slower than Rossby waves with narrow guides. A corresponding westward propagating wave front is readily observed in satellite altimetry of the Pacific [13] as well as the Atlantic [14] sea surface associated with wind-driven oceanic Rossby waves. Tidal Rossby modes approximately satisfying this wave guide equation are not well represented by plane waves in the latitudinal direction.

The wave dynamics given by Eqs. (3.8), (3.9) unify Margules' nondivergent Rossby waves with Matsuno's equatorial β-plane approximation. The underlying wave equation (3.6) is not really new. Its equatorial β-plane version is discussed in most text books on quasigeostrophic theory as a prototype of ageostrophic motion. What is different, though, is the demonstration that these ageostrophic dynamics provide a common basis for all Rossby modes of the generic tidal equation. This is clearly seen in Figs. 1(b) and 1(c): all Rossby frequencies are well approximated by Eq. (3.8).

The basic requirement for the identification of trapping regions of general wave-circulation systems is the consideration of the global domain. The spheroidal approximation (3.8), (3.9) of the Matsuno equation (3.6) exhibits essential features of an appropriate global Rossby filter of tidal dynamics: it applies on the entire spherical surface and captures the low-frequency Rossby and gravity modes of the tidal spectrum. However, due to the breakdown of this approximation for the Yanai mode at moderate Lamb parameters it has to be discarded as ambiguous with respect to stability conclusions.

Nevertheless, the key to the ageostrophic global Rossby wave dynamics of Eqs. (3.8), (3.9) is the neglibility of the r.h.s. of Eq. (3.6) due to the small divergence of these disturbances. In the limit $c \to \infty$ the generic tidal equations assume the form [27]

$$j^n;_n = 0, \tag{3.11}$$

$$d_t j_n + \epsilon_{mn} F j^m + \partial_n p = 0. \tag{3.12}$$

The only eigenmodes of Eqs. (3.11), (3.12) are divergence-free global Rossby waves. This limit represents the Margules filter of Laplace's tidal equation. Its space-time version [Eqs. (3.11), (3.12)] corresponds uniquely to the previously used Margules limit in wave number space and the related eigenfunctions of the generic tidal problem are Legendre functions. Thus, the Margules filter is well defined in space-time, wave number space, and in the function-space of the generic tidal operator. The basic wave mechanism in this regime is the imbalance of horizontal momentum disturbances and restoring Coriolis forces. As with all nondivergent fluid motion, pressure forces maintain a divergence-free mass flux. Moreover, the large-c limit does not impose restrictions or modifications on the underlying circulation. With its preservation of the global domain, its uniqueness in space-time, wave number space and function space the Margules limit [Eqs. (3.11), (3.12)] provides the geometrically and physically appropriate filter of tidal dynamics for the analysis of Rossby wave guide geographies of arbitrary circulations.

IV. ROSSBY WAVE GEOGRAPHY OF THE THERMAL WIND

It has been shown in the previous section that a mean circulation affects the wave guide geography. In the simple case of solid body rotation without available potential energy such modifications remain limited to changes of the width of the Yoshida guide. This section considers more significant alterations induced by a circulation with finite geostrophy and baroclinicity parameters. The governing equations of the basic wave-circulation system are the tidal equations of the thermal wind [Eqs. (2.12)–(2.15)]. Of particular climate relevance are low-frequency Rossby wave disturbances and the global Rossby wave-circulation system follows from Eqs. (2.12)–(2.15) by application of the Margules filter. This requires to consider the tidal equations of the thermal wind for

$$j^n;_n = (i^n + r j^n);_n = 0.$$

In terms of layer perturbations these conditions imply

$$(j^n_{(1)} + j^n_{(2)});_n = j^n_{(1)};_n = 0$$

so that also

$$j^n_{(2)};_n = 0.$$

In view of the dynamics of nondivergent Rossby waves it is hence convenient to transform Eqs. (2.12)–(2.15) from the bishallow representation to the 2-layer representation. This is obtained by appropriate linear combination of Eqs. (2.12)–(2.15) and one arrives at

$$d_{(\ell)} m_{(\ell)} + j^n_{(\ell)};_n = 0,$$

$$d_{(\ell)} j_n^{(\ell)} + \epsilon_{mn} F_{(\ell)} j^m_{(\ell)} + R_{(\ell)} \partial_n p_{(\ell)} = 0.$$

Here

$$d_{(\ell)} = \partial_t + U_{(\ell)} \partial_\lambda, \quad R_{(\ell)} = R_E^{(\ell)} (1 - b_{(\ell)} \sin^2\varphi)$$

with geostrophy parameters

$$b_{(\ell)} = R_0^{(\ell)}/R_E^{(\ell)} = a^2(2\Omega + U_{(\ell)}) U_{(\ell)} / \gamma_{(\ell)} R_E^{(\ell)}$$

while one finds for the pressure perturbation

$$p_{(1)} = \gamma_1 m_{(1)} + \gamma_2 m_{(2)}, \quad p_{(2)} = \gamma_2 (m_{(1)} + m_{(2)}) = \gamma_2 m.$$

With the Margules filter the layerwise mass flux perturbations can be represented in terms of stream functions $A_{(\ell)}$

$$j_n^{(\ell)} = \epsilon_{nm} \partial^m A_{(\ell)}$$

and the curl of the layerwise momentum budgets yields

$$[(R_{(\ell)} \Delta - \partial^a R_{(\ell)} \partial_a) d_{(\ell)} - \epsilon^{mn} R^2_{(\ell)} \partial_m Z_{(\ell)} \partial_n] A_{(\ell)} = 0.$$

For both layers these potential vorticity budgets have the same form and layer indices will therefore be dropped in the following. While divergent disturbances seperate the tidal equations of the thermal wind into barotropic and baroclinic subsystems, the Margules filter seperates the system with respect to layers: nondivergent Rossby waves propagate independently in individual layers with the mean vertical shear as the primary seperation-agent. The Rossby wave dynamics of the thermal wind are thus given by the dispersive and trapping characteristics of the nondivergent eigenmodes of two structurally identical systems of the form (3.1) with finite geostrophy parameters.

Since the mean potential vorticity gradient (2.9) of the geostrophic flow in an individual layer satifies

$$R^2\partial_n Z = R\partial_n F - F\partial_n R$$

the perturbation potential vorticity budget may be cast in the form

$$R(\Delta d_t - \epsilon^{ab}F_a\partial_b)A = D^{ab}R_b\partial_a A. \tag{4.1}$$

For vanishing available potential energy $(\partial_b R=0)$, Eq. (4.1) obviously reduces to the Margules wave equation of the generic tidal problem. In the following, the spectrum and wave geography of the full equation (4.1) will be considered. Assuming the stream function to be of the form (3.4) one obtains for Eq. (4.1)

$$v(\Delta + \tau M)A = -2(buy\partial_y - \tau M)A \tag{4.2}$$

with

$$u = 1-y^2, \quad v = 1-by^2.$$

To the author's knowledge an ordinary differential equation of this structure is not in the literature and its analysis has to employ approximate analytical methods in conjunction with numerical integrations. There are two alternative forms of this equation with advantages for specific questions. An obvious transformation casts Eq. (4.2) into the form

$$\left[v^2\partial_y \frac{u}{v}\partial_y - v\left(\frac{M^2}{u} - \tau M\right) - 2\tau M\right]A = 0 \tag{4.3}$$

clearly exhibiting the self-adjoint character of the wave operator. Secondly, introduction of the latitudinal coordinate

$$q = \int_0^y dx \quad 1/\sqrt{uv}$$

and transformation to the function

$$\Psi = u^{1/4}v^{-3/4}A$$

leads to the Schrödinger equation

$$(\partial_q^2 + E - V)\Psi = 0 \tag{4.4}$$

with eigenvalue

$$E = \frac{1}{2} - \frac{3}{2}b - \tau M - M^2$$

and the ''potential''

$$V(q) = bM\tau sn^2 - (1-b)\left[\frac{15}{4}bsd^2 - \left(M^2 - \frac{1}{4}\right)sc^2\right],$$

where

$$sn = sn(q|b)$$

and sd and sc correspondingly denote Jacobi's elliptic functions [25] of argument q and parameter b. It follows from Eq. (4.3) that the dispersion relation for Eq. (4.1) is of the form

$$\sigma = \sigma(N,M;b) = -M/\epsilon(N,M;b) \tag{4.5}$$

with (nondimensional) eigenfrequencies

$$\sigma = 1/\tau = (\omega_0 - UM)/2(\Omega + U)$$

and eigenvalue ϵ. Since the wave operator (4.3) is self-adjoint its spectrum is real and hence the eigenfrequencies of Eq. (4.1) are real. This is the statement of linear stability of the thermal wind [Eqs. (2.10), (2.11)] as well as the barotropic circulation with available potential energy (2.7)–(2.9) against nondivergent Rossby wave disturbances. It is stressed that this does not claim the linear stability of these wave-circulation systems in general. Kelvin-Helmholtz instability involves divergent baroclinic gravity waves and baroclinic instability is assumed to be due to divergent Rossby waves. Such disturbances are not included in Eq. (4.1).

From the Schrödinger equation (4.4) one obtains readily a general expression for the critical latitude

$$y_{\rm cr} = y_{\rm cr}(\sigma, M; b). \tag{4.6}$$

Setting

$$V(q_{\rm cr}) = E$$

and using the trigonometric representation of Jacobi's elliptic functions [25] one finds

$$b^2M\tau y_{\rm cr}^6 + ba_4 y_{\rm cr}^4 - a_2 y_{\rm cr}^2 - E = 0$$

with

$$a_4 = bM^2 + \frac{5}{2}(1-b) - bM\tau + 1$$

and

$$a_2 = 2bM^2 + \tau M - \frac{9}{4}(1-b)^2 + 2.$$

In this form, Eq. (4.6) is the general wave guide equation for nondivergent Rossby waves on a thermal wind. In the limit of solid body rotation: $b=0$ and the wave guide equation (4.6) reduces to

$$y_{\rm cr}^2 = \left(M^2 + M\tau - \frac{1}{2}\right) \Big/ \left(M\tau - \frac{1}{4}\right) \approx 1 + \sigma M$$

in agreement with the Margules limit $c \rightarrow \infty$ of the Matsuno wave guide equation (3.9). Minor discrepancies between both expressions are due to the fact that Eq. (4.6) refers to the function Ψ while Eq. (3.9) applies to the stream function A. If the layer thickness vanishes at the poles the geostrophy parameter assumes the value $b=1$ and the wave guide equation becomes

$$(y_{\rm cr}^2-1)(M\tau y_{\rm cr}^2+M\tau+M^2+1)=0$$

with two roots

$$y_{\rm cr}^2=1,\ \ y_{\rm cr}^2=-(M^2+M\tau+1)/M\tau\approx-(1+\sigma M).$$

For the second solution, $y_{\rm cr}$ will become imaginary indicating the absence of wave trapping but not an instability of the ground state. In the limit of low frequencies $\sigma\rightarrow 0$ the wave guide equation (4.6) reduces to the simple expression

$$y_{\rm cr}^2=1/|b|.$$

At large absolute values of the parameter b geostrophic circulations thus effect a pronounced regionalization of nondivergent low-frequency waves. The wave guide equation (4.6) alone does not provide information on which side of the critical latitude the wave function is oscillating. This issue requires consideration of the derivative of the potential $V(q)$ with respect to q at the critical latitude. However, the resulting expression is not very transparent and it is more convenient to use analytical approximations of Eq. (4.1) as well as numerical solutions.

Approximate analytical expressions for the eigenfunctions of Eq. (4.1) can be obtained in the limit of small absolute values of the geostrophy parameter. With $|b|\ll 1$ the first order Taylor expansion of v^{-1} yields for Eq. (4.2)

$$(\Delta-By^2-M\tau)A\approx 0, \tag{4.7}$$

where

$$B=2bM/\sigma$$

denotes the square of an effective Lamb parameter. This is a spheroidal wave equation. However, unlike the wave equations of the generic tidal problem, Eq. (4.7) is not necessarily prolate. Only if disturbances run with the wind: $bM>0$ and in this case, Eq. (4.7) is a prolate equation. On the other hand, for disturbances running against the wind: $bM<0$ and in this case, Eq. (4.7) is an oblate spheroidal wave equation [25,26]. Both cases differ significantly with respect to their wave guide geographies.

At $b=0$, the effective Lamb parameter also vanishes and Eq. (4.7) reduces to the classical Margules limit of exclusively westward propagating Rossby waves on a circulation without available potential energy. This system has been discussed in the previous section. As long as B remains small the stream function A behaves essentially as a Legendre function. However, although the approximation (4.7) is based on small absolute values of the geostrophy parameter b, the square of the effective Lamb parameter B can well become large particularly for low-frequency waves. If B is positive and large: $B\gg 1$ the stream function A is approximated by [26]

$$A=S_L^M(y;\sqrt{B})\approx u^{|M|/2}e^{-x^2/2}H_N(x),$$

where $H_N(x)$ is the Hermite polynominal of order $N=L-|M|$ and argument $x=yB^{1/4}$. This approximation captures the oscillatory and trapping characteristics of prolate spheroidal wave functions as shown in Fig. 2. For $B\gg 1$ application of the spheroidal operator (4.7) to this representation leads to the Hermite equation

$$\left(\partial_x^2-2x\partial_x+\frac{\epsilon_P-M^2}{\sqrt{B}}-1\right)H_N=0$$

and thus for the eigenvalue

$$\epsilon_P\approx(2N+1)\sqrt{B}+M^2.$$

Since the prolate spheroidal eigenvalue ϵ_P is positive it follows from Eq. (4.5) that M has to be negative and for B to be positive the geostrophy parameter b also has to be negative. Hence, in the prolate case, Eq. (4.7) represents nondivergent, westward propagating Rossby waves on westward winds such as the trades ($bM>0,b<0,M<0$). For the dispersion relation (4.5) this eigenvalue yields

$$\sigma M^2+(2N+1)\sqrt{2bM\sigma}+M=0$$

which is sufficiently approximated by

$$\sigma\approx M/2b(2N+1)^2 \tag{4.8}$$

at low frequencies. Similar to Matsuno's theory the critical latitude follows as

$$y_{\rm cr}^2\approx(2N+1)/\sqrt{B}. \tag{4.9}$$

In the prolate case, metric and circulation cooperate to establish an equator-centered wave guide geography. Pronounced equatorial trapping of divergence-free, westward propagating Rossby waves requires a strong westward circulation. The basic structure of this approximation closely resembles Matsuno's theory. However, in the present case the ''β-plane'' coordinate is given by $x=yB^{1/4}$. This definition becomes void if the geostrophy parameter b vanishes. In contrast to a mere tangential plane, regional approximations of the Matsuno-type rely on the wave geography of the underlying circulation.

For waves running against the wind the square of the effective Lamb parameter becomes negative: $B<0$ and the stream function is given by the oblate spheroidal wave function

$$A=S_L^M(y;i\sqrt{|B|}).$$

These functions are shown in Fig. 3. In the oblate case the competition of trapping effects due to the metric and the circulation generates equator- as well as pole-centered wave guides. The possibility of tidal dynamics at strictly imaginary Lamb parameters was first pointed out by Lindzen [12,22]. Longuet-Higgins [22] demonstrated that the generic tidal spectrum at imaginary Lamb parameters is real and the transition from prolate to oblate tidal dynamics *eo ipso* is not associated with instability. Since then oblate tidal dynamics

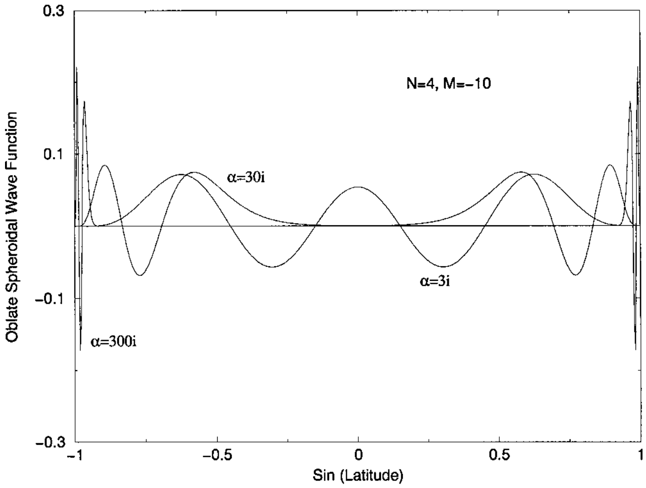

FIG. 3. Oblate spheroidal wave function. For $N=4$, $M=-10$ at Lamb parameters $\alpha=3i,30i,300i$.

have not received much attention primarily because the physics underlying oblate behavior remained essentially unclear. With spherical shallow water theory wave-circulation systems can be considered on the global domain and it emerges here that Rossby waves running against a geostrophic wind are governed by oblate tidal dynamics.

A major feature of oblate spheroidal wave functions is their degeneracy at large absolute values of the effective Lamb parameter [26]: at some moderate value of the imaginary Lamb parameter the eigenvalues of even and odd solutions coalesce (see Appendix, Figs. 7 and 8). At large absolute values of the imaginary Lamb parameter there are two spheroidal wave functions with identical eigenvalue. For large absolute values of the effective Lamb parameter oblate spheroidal wave functions are well approximated by [26]

$$S_L^M(y;i\sqrt{|B|})\approx u^{|M|/2}e^{-x/2}L_K^{|M|}(x),$$

where $L_K^{|M|}(x)$ is the generalized Laguerre polynominal of order $K=(L-|M|,L-|M|-1)/2$ if $(L-|M|)$ is (even, odd) and argument $x=2|B|^{1/2}(1-|y|)$. This representation accounts for significant wave amplitudes in the vicinity of the poles. While Hermite polynominals are known from the quantum oscillator, the Schrödinger wave function of quantum particles in a Coulomb field is given by generalized Laguerre polynominals [30]. Inserting this approximation into the spheroidal equation (4.7) one arrives with $|B|\gg 1$ at the Laguerre equation

$$\left(x\partial_x^2+(|M|+1-x)\partial_x+\frac{\epsilon_O-B}{4\sqrt{|B|}}-\frac{|M|+1}{2}\right)L_K^{|M|}=0$$

and obtains for the eigenvalue

$$\epsilon_O=B+2N\sqrt{|B|},$$

where $N=2K+|M|+1$ is given by $(L+1,L)$ if $(L-|M|)$ is (even, odd). With Eq. (4.5) this eigenvalue yields the dispersion relation

$$\sigma=-M/8bN^2 \tag{4.10}$$

for nondivergent Rossby waves propagating against a geostrophic wind with available potential energy. Since the oblate spheroidal eigenvalue is not necessarily positive (see Appendix, Figs. 7 and 8) two cases have to be distinguished. For

$$\sigma>|bM|/2N^2$$

the oblate eigenvalue ϵ_O is positive. According to Eq. (4.5) the zonal wave number M has to be negative in this case and for B to be negative the geostrophy parameter b has to be positive. Hence, this regime applies to westward propagating Rossby waves on an eastward wind ($bM<0,b>0,M<0$). On the other hand, at very low frequencies

$$\sigma<|bM|/2N^2$$

the oblate eigenvalue ϵ_O is negative and zonal wave numbers M have to be positive while geostrophy parameters b are negative. This case represents eastward propagating Rossby waves on a westward wind ($bM<0,b<0,M>0$). Unlike the generic tidal problem the tidal equation of the geostrophic wind with available potential energy also admits eastward propagating Rossby waves at very low frequencies. Formally these eigenmodes are a consequence of negative oblate spheroidal eigenvalues. The oblate wave guide geography of the Laguerre-limit of Eq. (4.7) follows now much the same way Bohr's quasiclassical atomic theory follows from the quantum mechanics of a Coulomb particle [30]. For $x/2\gg 1$, stream functions basically decrease exponentially and one obtains thus for the width of the pole-centered wave guide

$$1-|y_{\rm cr}|\approx 1/\sqrt{|B|}=1/4|b|N, \tag{4.11}$$

where the dispersion relation (4.10) has been used in the second equation. At small geostrophy parameters, higher modes of Rossby waves running against the wind are trapped in the vicinity of the pole. For small absolute values of b, large-B approximations to Eq. (4.7) in the oblate as well as in the prolate case apply essentially at large mode numbers N. Similar to the Hermite approximation for the Yoshida guide, the Laguerre approximation becomes meaningless if the polar wave guide vanishes physically.

The spheroidal approximation (4.7) to the wave equation (4.1) provides a qualitative overview of the dynamics of nondivergent Rossby waves on a circulation with small geostrophy parameter. A more detailed quantitative picture of the wave dynamics of nondivergent Rossby waves on a geostrophic flow is obtained by numerical integration of Eq. (4.1). These integrations are not restricted to weakly geostrophic circulations. The employed code evaluates a discretized version of Eq. (4.3) with 400 points in the interval $y\epsilon[-1,1]$ using NAG-Lib routine F02GJE for geostrophy parameters $b\leqslant 1$. Figure 4(a) shows the Matsuno representation of the dispersion relation for geostrophy parameters $b=-3,0,1$, while the Lamb representation for $M=-4,-1,1$ is given in Fig. 4(b).

The middle panel of Fig. 4(a) with $b=0$ represents Margules' Rossby modes of the generic dispersion relation (3.7) and is here given for reference purposes. Numerically calculated antisymmetric solutions of Eq. (4.1) for westward Rossby waves on an eastward circulation with $b=1$ are

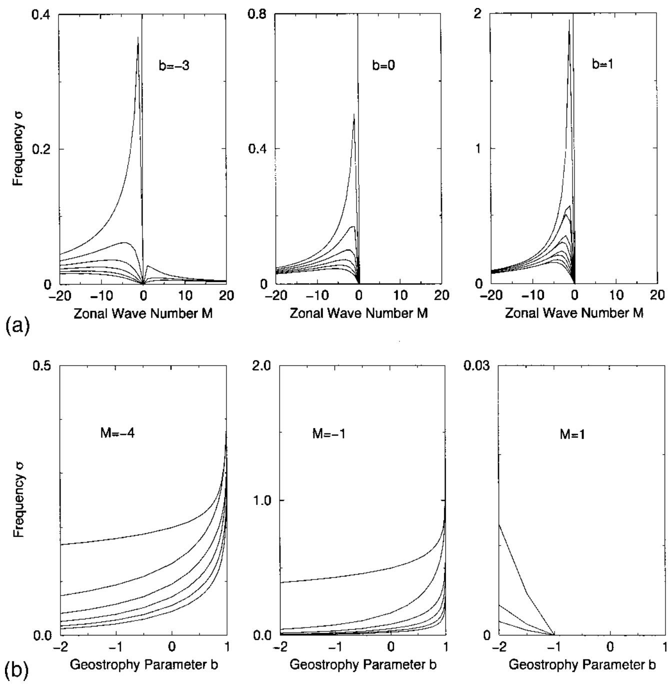

FIG. 4. (a). Rossby wave frequencies. Matsuno representation at geostrophy parameters $b=-3,0,1$. (b) Rossby wave frequencies. Lamb representation for zonal wave numbers $M=-4,-1,1$.

shown in Fig. 5. The right panel of Fig. 4(a) as well as the left ($M=-4$) and central ($M=-1$) panel of Fig. 4(b) show that the spectrum at $b=1$ exhibits the characteristic oblate coalescence of eigenfrequencies. Figure 4 demonstrates furthermore that sufficiently large positive geostrophy parameters (eastward circulation) lead to the emergence of Rossby waves with frequencies exceeding the Lamb parameter: $\sigma>1$. As such high-frequency Rossby modes are excluded in generic tidal dynamics their appearance here is a sole consequence of the finite available potential energy of the circulation.

The left panel ($b=-3$) of Fig. 4(a) and the right panel ($M=1$) of Fig. 4(b) show very low eigenfrequencies of eastward propagating Rossby waves. It is emphasized that for each eigenfrequency at a positive zonal wave number there

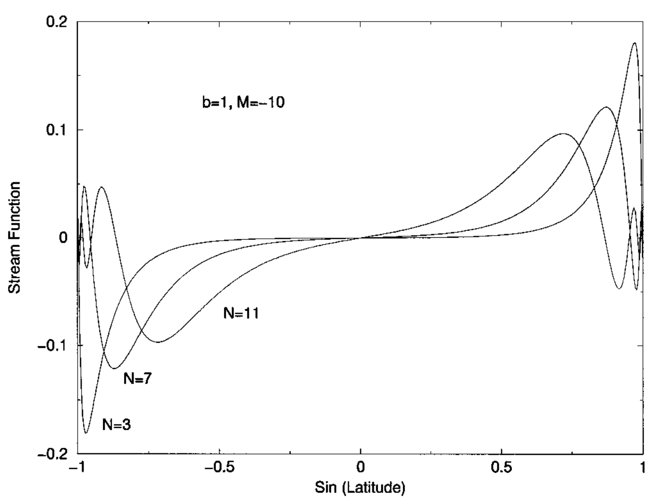

FIG. 5. Stream function of pole-trapped, westward Rossby waves on eastward circulation.

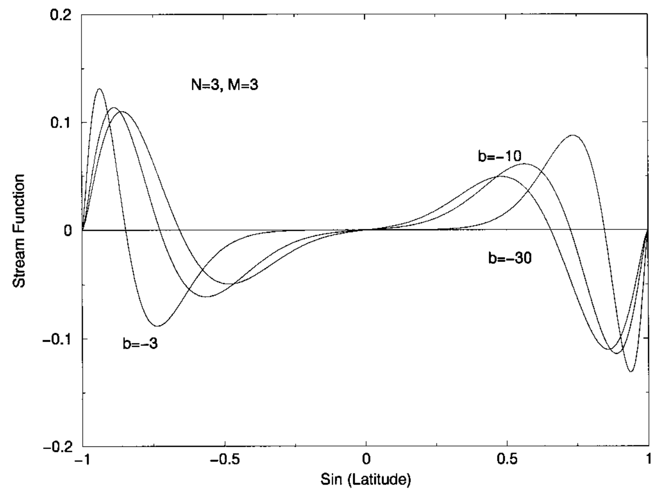

FIG. 6. Stream function of pole-trapped, eastward Rossby waves on westward circulation.

exist two eigensolutions: an eigenfunction which is symmetric with respect to the equator as well as an antisymmetric eigenfunction. Antisymmetric solutions of Eq. (4.1) at negative eigenvalues are shown in Fig. 6 clearly exhibiting the pole-trapped nature of these solutions. Eastward propagating Rossby waves are exclusively due to the finite available potential energy of the westward circulation. Eastward Rossby waves (i.e., negative eigenvalues), degeneracy and polar trapping are characteristic features of oblate spheroidal wave functions. Figures 5 and 6 show that the oblate trapping characteristics of Eq. (4.1) at large absolute values of b differ from those at small geostrophy parameters. Pole-centered wave guides become wider as the absolute value of b and the mode number N increase.

The combination of analytical approximations and numerical integrations provides a comprehensive overview of the eigensolutions of Eq. (4.1). A sufficiently strong geostrophic circulation with available potential energy significantly affects the regional distribution of Rossby wave amplitudes. Westward waves propagating on a westward wind are trapped in an equator-centered wave guide. Westward waves on an eastward wind can have high frequencies $\sigma>1$ and are trapped in a pole-centered wave guide. Westward winds allow very low-frequency eastward propagating Rossby waves trapped in the vicinity of the poles. Matsuno-type regional approximations exist for the interior of the equatorial as well as the polar wave guide.

Westward Rossby waves on westward trade winds are widely observed in the tropical troposphere. The effect of the intensity of the trades on the meridional width of these disturbances is governed by Eq. (4.1). For Rossby waves in the tropical ocean the mean circulation plays a minor role and these disturbances are sufficiently represented by generic Matsuno theory. At higher latitudes, the circulation of the troposphere as well as the antarctic ocean is essentially eastward and disturbances propagate generally with the flow. Equation (4.1) does not represent wave-circulation systems of this type. In these cases the inclusion of divergent disturbances is necessary. For the high latitude stratosphere, the spectrum of Rossby waves propagating against the wind is not known at this time.

V. SUMMARY

The mathematical physics of global wave-circulation systems are given by spherical shallow water theory. The tidal equations of the thermal wind govern the small-amplitude dynamics of a bifluid in a non-Euclidean geometry. Metric and Coriolis forces on one hand and the circulation on the other cooperate and compete in establishing the system's inhomogenity and anisotropy. The resulting background structure effects a pronounced regionalization of low-frequency disturbances. The dynamics of equator-trapped waves closely resemble quantum mechanics in a potential well while pole-trapped waves behave similar to atomic particles in a Coulomb field. Various transport mechanisms of the climate system globalize regionally confined variability.

Earth's climate is primarily forced by differential solar heating. This forcing supplies the global circulation with available potential energy. The spherical shallow water equations admit simple stationary, zonal and geostrophic solutions with available potential energy. In the barotropic case these solutions form a one-parameter family where the geostrophy parameter essentially coincides with the climatological NAO-index. Finite available potential energy does not require the circulation to be baroclinic. For the bishallow fluid, corresponding thermal wind solutions form a two-parameter family. In addition to the geostrophy parameter, a thermal wind is characterized by a baroclinicity parameter measuring the vertical shear in terms of the amplitude of the baroclinic pressure gradient. Linearization of the bishallow water equations around such a stationary circulation yields the tidal equations of the thermal wind. These equations govern the dynamics of small amplitude disturbances of a stably stratified, stationary, zonal, geostrophic and vertically sheared circulation with available potential energy. In spite of their relative simplicity the tidal equations of the thermal wind address a wide range of essential dynamical issues of the climate system. In addition to the propagation of barotropic and (first mode) baroclinic gravity and Rossby waves they determine the linear stability of the thermal wind as well as the regional distribution of wave activity.

The distinguishing feature of wave dynamics on the global scale is the regionalization of low-frequency disturbances. Spatial variability of the metric, the Coriolis forces and the circulation generate an inhomogeneous and anisotropic background that traps low-frequency waves in zonally oriented wave guides. In addition to the spectrum, global wave dynamics are thus characterized by a wave guide geography. For the generic tidal problem the regionalization of wave activity is determined by the equator-centered Yoshida guide. Depending on frequency, this wave guide extends to moderate and high latitudes. In the vicinity of the critical latitude, tidal eigenfunctions differ significantly from plane waves. At this time, wave-circulation theory still lacks the complete analytical solution of the generic tidal problem. On the entire wave number space, approximate analytical solutions in terms of Lamé-type spheroidal wave functions are known. In special cases, exact analytical solutions can be represented in terms of these functions. At large Lamb parameters spheroidal approximations coincide with Matsuno's equatorial β-plane theory. Unlike an arbitrary tangential plane, this concept approximates the interior of the Yoshida guide and becomes void if the wave guide vanishes physically. An ageostrophic spherical Matsuno equation unifies Margules' nondivergent Rossby waves with Matsuno's theory. This unification represents all Rossby modes of the generic tidal spectrum. The unique and covariant Rossby filter of tidal dynamics is given by Margules' large-c limit. This filter eliminates all but low-frequency, ageostrophic, nondivergent Rossby modes from the tidal equations. As it retains the global domain of tidal dynamics, the Margules filter is appropriate to determine the global Rossby wave guide geography of general circulation systems.

The Margules filter decomposes the tidal equations of the thermal wind into two independent layer subsystems with the vertical shear as the major separation agent. Rossby wave dynamics on the thermal wind are thus determined by the spectrum and wave geography of the nondivergent eigenmodes of two structurally identical tidal equations with available potential energy. Both layers and thus the thermal wind are linearly stable against nondivergent Rossby wave disturbances. The wave guide geography of the thermal wind is determined by the cooperation and competition of trapping effects due to surface curvature and Coriolis forces on one hand and the circulation on the other. In the prolate case curvature and Coriolis forces cooperate with the circulation in establishing an equator-centered wave guide. A westward circulation enhances equatorial trapping of westward propagating, divergence-free Rossby waves. In the oblate case curvature and Coriolis forces compete with the circulation and both, equator-centered as well as pole-centered wave guides are possible. Oblate dynamics govern nondivergent Rossby waves propagating against the wind. For sufficiently strong circulations these Rossby waves are trapped in a pole-centered wave guide. Westward circulations admit very low-frequency eastward propagating Rossby waves while westward Rossby waves on intenser eastward circulations exhibit frequencies in excess of the Lamb parameter. Oblate degeneracy admits symmetric as well as antisymmetric modes at the same eigenfrequency. Regional approximations in terms of orthogonal polynominals exist for both, prolate and oblate wave guide geographies. In the prolate case wave functions inside the Yoshida guide are approximated by Hermite polynominals essentially corresponding to Matsuno's theory. Inside the polar wave guide, on the other hand, wave functions are approximated in terms of generalized Laguerre polynominals. Both approximations depend on the physical existence of the wave guide.

The present paper demonstrated the regionalization of nondivergent eigenmodes on a circulation with available potential energy. The inclusion of divergent eigenmodes will also raise the issue of instabilities and their geography. While the results of this study imply a regionalization of the susceptibility to wave growth, the variability of the circulation is generally global in nature. From El Nino dynamics inside the oceanic Yoshida guide it is well known that coastally trapped Kelvin waves as well as atmospheric teleconnections provide modes of globalization for regionally confined variability. Complete global variability patterns are determined by the composite effect of wave activity as well as advective and diffusive transports.

APPENDIX: SPHEROIDAL WAVE FUNCTIONS

In contrast to functions of the hypergeometric type, the literature on spheroidal wave functions is not very extensive [26,31,32]. Basic properties are given in Ref. [25]. Prolate spheroidal wave functions $S_L^M(y;\alpha)$ of integer degree L and order M satisfy the equation

$$\left[\partial_y(1-y^2)\partial_y-\frac{M^2}{1-y^2}-\alpha^2y^2+\epsilon_P\right]S_L^M(y;\alpha)=0$$

for real Lamb parameters α and remain regular at the poles $y=\pm 1$. At small values of α, prolate spheroidal wave functions behave as Legendre functions

$$S_L^M(y;\alpha^2\ll 1)\approx P_L^M(y)$$

while they are approximated by Hermite polynominals at large α

$$S_L^M(y;\alpha^2\gg 1)\approx(1-y^2)^{|M|/2}e^{-x^2/2}H_N(x)$$

with argument $x=y\sqrt{|\alpha|}$ and order $N=L-|M|$. At fixed degree and order numerical solutions of the prolate spheroidal wave equation are shown in Fig. 2 for varying α. The Lamb parameter is seen to control the wave guide characteristics.

For the function

$$F(y;\alpha)=(1-y^2)^{-1/2}S_L^M(y;\alpha)$$

the prolate spheroidal wave equation yields the wave guide equation

$$\alpha^2y_{\rm cr}^4-(\alpha^2+\epsilon_P)y_{\rm cr}^2+\epsilon_P-M^2+1=0$$

with the solution

$$2\alpha^2y_{\rm cr}^2=\alpha^2+\epsilon_P\pm\sqrt{(\alpha^2-\epsilon_P)^2+4\alpha^2(M^2-1)}$$

and the limit

$$y_{\rm cr}^2=(\epsilon_P-M^2+1)/\epsilon_P$$

at $\alpha=0$. The critical latitude decreases with increasing Lamb parameter. In the vicinity of the critical latitude the function F satisfies the Airy-type equation

$$[(1-y_{\rm cr}^2)\partial_x^2-Wx]F\approx 0$$

with $x=y-y_{\rm cr}$ and

$$W(y_{\rm cr})=2y_{\rm cr}\left(\frac{M^2-1}{(1-y_{\rm cr}^2)^2}+\alpha^2\right).$$

For finite M the inequality

$$Wx<0$$

always holds if $y^2<y_{\rm cr}^2$ and hence F oscillates exclusively equatorwards of the critical latitude. The prolate spheroidal wave equation only admits an equator-centered wave guide.

A closed expression for the prolate spheroidal eigenvalue is not known. If α is small

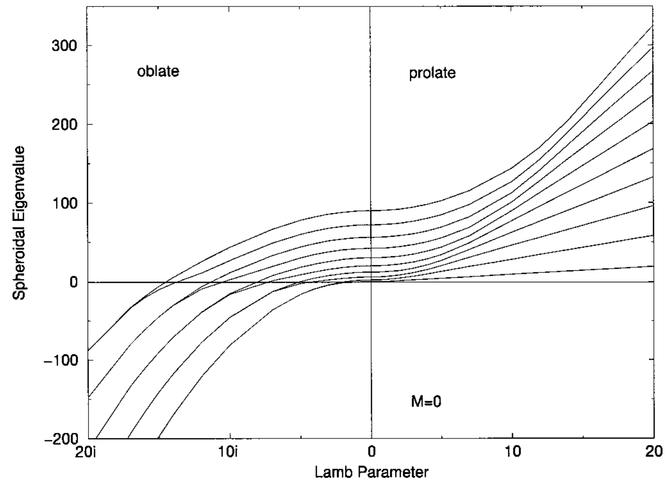

FIG. 7. Spheroidal eigenvalues. Lamb representation for $M=0$.

$$\epsilon_P(L,M;\alpha^2\ll 1)\approx L(L+1)+O(\alpha^2)$$

while at large values of the Lamb parameter

$$\epsilon_P(L,M;\alpha^2\gg 1)\approx(2N+1)|\alpha|+M^2+O(|\alpha|^0).$$

For all values of α the prolate eigenvalue exhibits the symmetry

$$\epsilon_P(L,M;\alpha)=\epsilon_P(L,-M;\alpha).$$

Numerically calculated prolate spheroidal eigenvalues at fixed zonal wave number $M=0$ are shown in the right panel of Fig. 7 while the left panel of Fig. 8 shows prolate eigenvalues at $\alpha=10$ for varying zonal wave number.

Oblate spheroidal wave functions $S_L^M(y;i\overline{\alpha})$ of integer degree L and order M satisfy the equation

$$\left[\partial_y(1-y^2)\partial_y-\frac{M^2}{1-y^2}-\alpha^2y^2+\epsilon_O\right]S_L^M(y;\alpha)=0$$

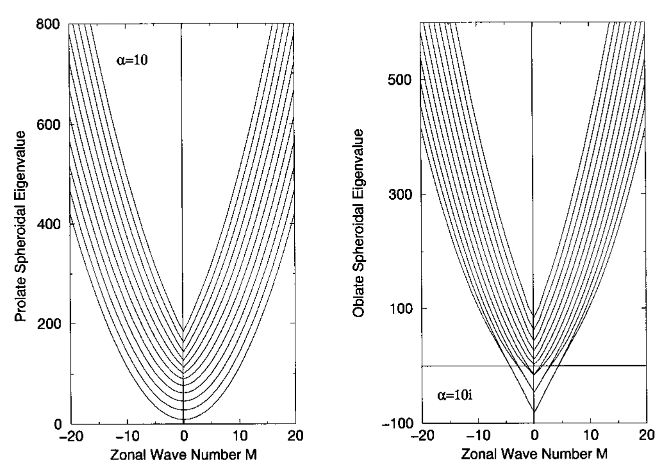

FIG. 8. Spheroidal eigenvalues. Matsuno representation. Left panel: prolate eigenvalues at $\alpha=10$. Right panel: oblate eigenvalues at $\alpha=10i$.

for Lamb parameters $\alpha = i\bar{\alpha}$ with real $\bar{\alpha}$ and remain regular at the poles $y=\pm 1$. At small values of α oblate wave functions behave like Legendre functions while they are approximated by generalized Laguerre polynominals

$$S_L^M(y;\alpha^2 \ll -1) \approx (1-y^2)^{|M|/2} e^{-x/2} L_K^{|M|}(x)$$

at large absolute values of α with argument $x = 2|\alpha|(1-|y|)$ and $K=(L+1,L)$ if $(L-|M|)$ is (even, odd). At fixed degree and order numerical solutions of the oblate spheroidal wave equation are shown in Fig. 3 for varying values of α. For the function

$$F(y;\alpha) = (1-y^2)^{-1/2} S_L^M(y;\alpha)$$

the oblate spheroidal wave equation yields the wave guide equation

$$\bar{\alpha}^2 y_{\rm cr}^4 - (\bar{\alpha}^2 - \epsilon_O) y_{\rm cr}^2 - \epsilon_O + M^2 - 1 = 0$$

with the solution

$$2\bar{\alpha}^2 y_{\rm cr}^2 = \bar{\alpha}^2 - \epsilon_O \pm \sqrt{(\bar{\alpha}^2 + \epsilon_O)^2 - 4\bar{\alpha}^2 (M^2-1)}$$

and the limit

$$y_{\rm cr}^2 = (\epsilon_O - M^2 + 1)/\epsilon_O$$

at $\alpha=0$. Complex solutions of the oblate wave guide equation are possible. However, as all solutions outside the real interval $[-1,1]$ they indicate nothing but the absence of wave trapping. In the vicinity of the critical latitude the function F satisfies the Airy-type equation

$$[(1-y_{\rm cr}^2)\partial_x^2 - Wx]F \approx 0$$

with $x = y - y_{\rm cr}$ and

$$W(y_{\rm cr}) = 2y_{\rm cr}\left(\frac{M^2-1}{(1-y_{\rm cr}^2)^2} - \bar{\alpha}^2\right).$$

This expression indicates that the trapping characteristics of the oblate equation are more complex than in the prolate case. At small α and large M oblate spheroidal functions are trapped in an equator-centered wave guide. On the other hand, at large values of α oblate spheroidal functions are trapped in a pole-centered wave guide.

Oblate spheroidal eigenvalues are real and a closed expression for $\epsilon_O(L,M;\alpha)$ as function of its arguments is not known. If α is small

$$\epsilon_O(L,M;(i\alpha)^2 \gg -1) \approx L(L+1) + O(\alpha^2)$$

while at large values of α

$$\epsilon_O(L,M;\alpha^2 \ll -1) \approx -\bar{\alpha}^2 + \bar{\alpha} N.$$

For all values of α the oblate eigenvalue exhibits the symmetry

$$\epsilon_O(L,M;\alpha) = \epsilon_O(L,-M;\alpha).$$

Numerically calculated oblate spheroidal eigenvalues at fixed zonal wave number $M=0$ are shown in the left panel of Fig. 7 while the right panel of Fig. 8 shows oblate eigenvalues at Lamb parameter $10i$ for varying zonal wave number. Two major features of the oblate spheroidal spectrum are noteworthy. The oblate spheroidal wave operator possesses negative eigenvalues. In the text these negative eigenvalues are responsible for eastward propagating Rossby waves. Secondly, the spectrum is degenerate. At sufficiently large absolute values of the Lamb parameter even and odd eigenmodes coalesce or merge and an eigenvalue is no longer associated with a definite symmetry of the corresponding eigenfunction with respect to the equator.

[1] P. Laplace, Mem. Acad. R. Sci. Paris **9**, 75 (1778).
[2] W. Kelvin, Proc. R. Soc. Edinburgh **10**, 92 (1879).
[3] K. Wyrtki, J. Phys. Oceanogr. **5**, 572 (1975).
[4] D. Neelin and M. Latif, Phys. Today **12**, 32 (1998).
[5] K. Yoshida, J. Oceanogr. Soc. Jpn. **15**, 159 (1959).
[6] T. Matsuno, J. Meteorol. Soc. Jpn. **44**, 23 (1966).
[7] L. Landau and E. Lifshitz, *Course of Theoretical Physics* (Pergamon, Oxford, 1978), Vol. 8.
[8] A. Gill, *Atmosphere-Ocean Dynamics* (Academic, London, 1982).
[9] E. Lorenz, Tellus **7**, 157 (1955).
[10] L. Richardson, *Weather Prediction by Numerical Process* (Cambridge University Press, Cambridge, 1922).
[11] L. Landau and E. Lifshitz, *Course of Theoretical Physics* (Pergamon, Oxford, 1975), Vol. 2.
[12] S. Chapman and R. Lindzen, *Atmospheric Tides* (Reidel, Dordrecht, 1970).
[13] G. Jacobs *et al.*, Nature (London) **370**, 360 (1994).
[14] P. Le Traon and J. Minster, J. Geophys. Res. **98**, 12 315 (1993).
[15] D. Müller, Phys. Rev. A **45**, 5545 (1992).
[16] P. Swarztrauber and A. Kasahara, SIAM (Soc. Ind. Appl. Math.) J. Sci. Stat. Comput. **6**, 464 (1985).
[17] G. Walker and E. Bliss, Mem. R. Met. Soc. **4**, 53 (1932).
[18] J. Hurrell, Science **269**, 676 (1995).
[19] H. Kuo, Adv. Appl. Mech. **13**, 247 (1973).
[20] N. Phillips, Tellus **6**, 273 (1954).
[21] D. Müller, Int. J. Mod. Phys. B **11**, 223 (1997).
[22] M. Longuet-Higgins, Philos. Trans. R. Soc. London, Ser. A **262**, 511 (1968).
[23] M. Yanai and T. Maruyama, J. Meteorol. Soc. Jpn. **44**, 291 (1966).
[24] M. Münnich and M. Latif (unpublished).
[25] M. Abramowicz and I. Stegun, *Handbook of Mathematical Functions* (Dover, New York, 1972).
[26] C. Flammer, *Spheroidal Wave Functions* (Stanford University Press, Sanford, 1957).
[27] M. Margules Sitzungsber, Kais. Akad. Wiss. Wien Math. Naturwiss. **102**, 11 (1893).
[28] D. Müller and J. O'Brien, Phys. Rev. E **51**, 4418 (1995).
[29] J. Bjerknes, Mon. Weather Rev. **97**, 163 (1969).
[30] L. Landau and E. Lifshitz, *Course of Theoretical Physics* (Pergamon, Oxford, 1977), Vol. 3.
[31] J. Meixner und F. Schäfke, *Sphäroidfunktionen* (Springer, Berlin, 1954).
[32] F. Arscott, *Periodic Differential Equations* (Macmillan, New York, 1964).